Measurement of ion energy distributions using a combined energy and mass analyzer

S. G. Walton, R. F. Fernsler, and D. Leonhardt
Plasma Physics Division, U.S. Naval Research Laboratory, Washington, DC 20375

(Received 22 March 2007; accepted 16 July 2007; published online 20 August 2007)

A method is described for measuring ion energy distributions using a commercially available, combined energy analyzer/mass spectrometer. The distributions were measured at an electrode located adjacent to pulsed, electron beam-generated plasmas produced in argon. The method uses energy-dependent tuning and was tested for various plasma conditions. The results indicate an improved collection efficiency of low-energy ions when compared to conventional approaches in measuring ion energy distributions. © *2007 American Institute of Physics.*
[DOI: 10.1063/1.2769352]

I. INTRODUCTION

Interrogating the flux of ions and neutrals at the surface of electrodes is an important diagnostic in the characterization of plasmas. For plasmas used in the processing of materials, both species identification and the determination of incident ion energies are particularly important. Devices that combine ion energy analyzers with mass spectrometers have been in existence for many years,[1] but the commercial availability of these devices has increased their popularity over the last decade or so. Generally, these systems consist of ion optics, an electrostatic energy analyzer, a quadrupole mass analyzer, and an ionizer to detect neutral species. Ions and neutrals are sampled through a small hole in an electrode and the entire system is differentially pumped to provide mean free paths that exceed the length of the device. The utility of these tools is their ability to mass and energy resolve the flux of ion species, which yield either a mass-resolved ion energy distribution or an energy-resolved ion mass distribution.

Despite this clear advantage, care must be taken when collecting and interpreting the data and several nuances must be considered when operating these devices.[2] Investigators have long worried about sampling plasma species through small orifices[3–7] since the sampling orifice diameter and depth can indluence the sheath, affect ion-neutral collisions on the analyzer side of the electrode, perturb ion trajectories, and/or reduce the ion current via neutralization on the walls. Most of these issues can be minimized by choosing an orifice with a small diameter and aspect ratio. Generally, the diameter should be a fraction of the sheath thickness and larger than the depth.

Of additional concern is the acceptance angle of the device, which is the largest angle (with respect to the surface normal) for which incident ions can be detected. The acceptance angle will have limitations determined by the geometry of the device[8] and an energy dependence,[9] due to the fact that collection efficiency of ions will vary with energy for a given set of *tuning conditions*, used here to describe the potential on all ion electro-optical elements. In the limit where the collection efficiency is the same for all energies, the acceptance angle will be limited only by geometry.

To better understand the energy dependence and how it can affect the measured energy distribution, first consider an ion energy distribution measured at a ground electrode. Neglecting the presheath, the range of energies will depend on ion collisions within the sheath. Ions that suffer no collisions realize the full sheath potential and arrive highly anisotropic, while ions at the low-energy end of the distribution experience some number of collisions and tend to be less anisotropic. An angular spread can also be introduced by the field distortion at the orifice,[6,10] which are dependent on orifice diameter-to-sheath width ratio; the larger the ratio, the larger the distortions. In this case, it is the lower energy ions which are most likely to be deflected by the fields at the orifice. It is not surprising then that the tuning conditions for low- and high-energy ions will be different. Typically, however, tuning conditions are determined using the most probable energy of the energy distributions, an energy that is frequently commensurate with the plasma potential. These tuning conditions are likely to be unsuitable for ions with lower energies, particularly if the sheath is highly collisional or there are significant field distortions at the orifice.

In this work, we used a modulated, electron beam-generated plasma produced in argon to develop a method to measure the ion energy distribution using a commercial, dual energy analyzer/mass spectrometer. We show the effect of the tuning conditions on the measured ion energy distributions and adopt a phenomenalistic approach to improve the collection efficiency over all energies and then use simple modeling to understand the results. The flux of ions incident to grounded electrodes adjacent to pulsed, electron beam-generated plasmas will vary in time, but the incident ion energies are generally low (5 eV).[11] These plasmas thus provide an interesting range of flux conditions and are useful in determining the collection efficiency of the device at near-zero ion energy.

 © 2007 American Institute of Physics

Downloaded 20 Aug 2007 to 132.250.158.37. Redistribution subject to AIP license or copyright, see http://rsi.aip.org/rsi/copyright.jsp

II. EXPERIMENT

A. Plasma chamber and production

The experimental apparatus, also described elsewhere,[12] is shown in the schematic of Fig. 1. The system vacuum was maintained by a 2000 l/s turbomolecular pump. High purity argon (99.999%) was introduced by a mass flow controller [50 SCCM (SCCM denotes cubic centimeter per minute at STP)] and the operating pressure of 50 mTorr was achieved by throttling the turbo pump. A beam of energetic electrons was produced by a linear hollow cathode[13] pulsed to 2 kV for 6 ms at a 20% duty factor. The emergent beam passed through a slot in a grounded anode and was then terminated at a second grounded anode located further downstream. The electron beam volume between the two anodes defines the ionization source volume, with the dimensions set by the slot size $(1\times 25\ \mathrm{cm}^2)$ and the anode-to-anode length (43 cm). Beam spreading from collisions with the neutral background was strongly limited by a longitudinal magnetic field of 150 G that was produced by a set of external magnetic field coils (not shown in Fig. 1). From Ref. 14, the employed field keeps the expansion of a 2 keV electron beam in 50 mTorr to <0.5 cm at the termination anode.

Electron beam produced plasmas are typically characterized by high plasma densities n_p and low electron temperatures T_e, although both quantities vary significantly over the course of one period when the plasma is modulated. As a reference, $n_p\sim 10^{11}\ \mathrm{cm}^{-3}$ while T_e is approximately 1.0 eV, measured on the axis of the electron beam plasmas produced in 50 mTorr argon.[12] The resulting ion energies at surfaces located adjacent to the plasma source thus range from 0 to about 5 eV.

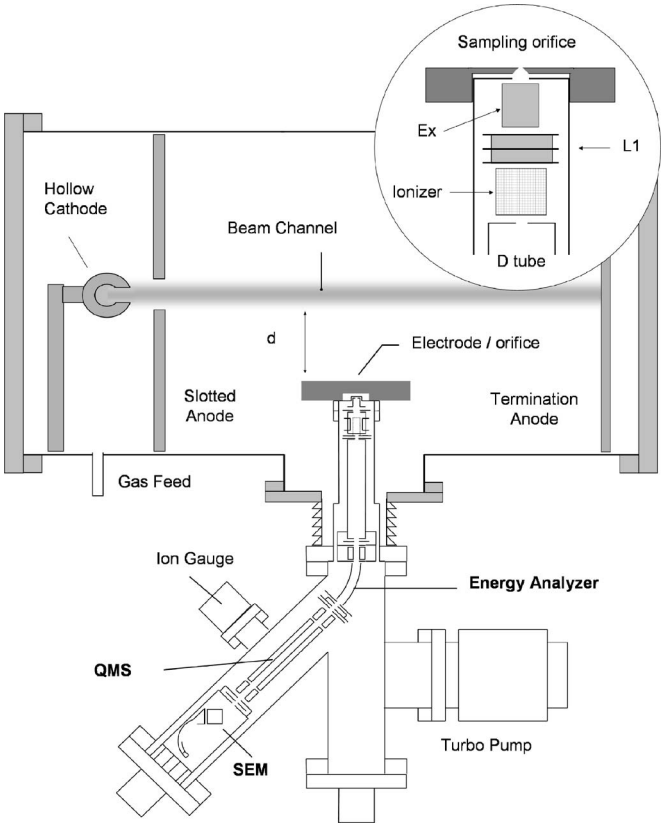

FIG. 1. Schematic of the system with inset showing detail of EQP entrance with the orifice, extractor (Ex), lens 1 (L1), ionizer, and drift tube (D tube). Not shown are magnetic field coils that surround the chamber.

B. Diagnostics

The dual energy analyzer/mass spectrometer is a Hiden EQP 300 plasma probe[15] and is shown in Fig. 1. Ions enter the EQP through a 20 μm diameter orifice located in the center of a grounded 5.7 cm diameter stainless steel electrode, which is mounted on the front of the EQP. The ions then pass through series of electrostatic lenses, an ionizer for neutral analysis, a 45° sector-field energy analyzer, and a quadrupole mass spectrometer (QMS), before collection by a secondary electron multiplier (SEM). The EQP is differentially pumped by a 150 l/s turbomolecular pump to eliminate collisions as ions propagate the length of the probe. For a pressure of 50 mTorr in the chamber, the pressure in the EQP remains below 10^{-6} Torr. The housing of the EQP is made of high permeability metal, to eliminate any effect the magnetic fields have on the ion trajectories inside the EQP.

The components of the EQP that are important to this work are the electrostatic lenses and energy analyzer. The lenses prior to the energy analyzer can be considered as two sections: an extraction region and a drift region. The extraction region (see Fig. 1, inset) consists of an extraction lens (extractor) and Einzel lens (lens 1) that serve to focus the ions into the drift region. In the drift region, ions are accelerated (or decelerated) by a specified potential and only those ions with the correct final energy $E=E_t\pm\Delta E/2$ will pass the energy analyzer. For the energy analyzer, ΔE increases with increasing E_t, and given the low ion energies measured in this work, E_t was set to 10 eV to provide a ΔE of approximately 0.3 eV, i.e., an uncertainty in energy of ±0.15 eV.[16] The initial ion energy at the orifice can thus be determined knowing the accelerating (decelerating) voltage within the drift region.

After exiting the energy analyzer, the monoenergetic beam of ions enters the QMS. The QMS passes only those ions with the correct mass-to-charge ratio and delivers them to the SEM for final detection. The SEM has not been calibrated to determine the absolute flux of each species, so only the intensity of the measured signal is reported.

Because the system uses a modulated plasma, all data were time resolved and our approach has been described previously.[12] Briefly, the SEM was gated such that the measured energy distributions were only accumulated during the designated time span. To increase the signal intensity and improve the signal to noise ratio, the count rate at a selected energy was acquired over ten gating windows (or plasma periods).

Data acquisition with the EQP was controlled via computer interface with vendor-provided software that allows for broad control over instrument operation. This includes setting and scanning the electro-optical element potentials individually or scanning multiple electro-optical elements in sequence via user-defined, automated routines.

Downloaded 20 Aug 2007 to 132.250.158.37. Redistribution subject to AIP license or copyright, see http://rsi.aip.org/rsi/copyright.jsp

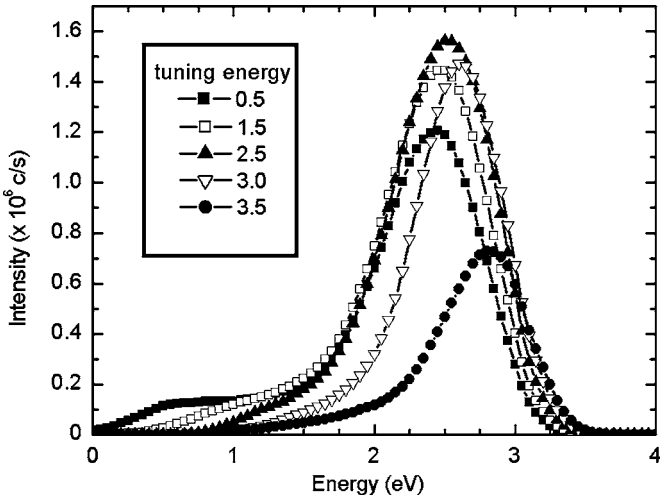

FIG. 2. Ar^+ ion energy distributions acquired after maximizing the signal intensity at the indicated tuning energy.

C. Simulations

SIMION (Ref. 17) software was used to simulate ion trajectories inside the EQP. Schematic diagrams of the EQP from Hiden Analytical were used to build an electrode array that approximates the internal arrangement of the ion optics up to the energy analyzer. Since the focus of the work is on energy dependence, transmission through and past the energy analyzer was assumed to occur if ions reached the front of the energy analyzer.

III. RESULTS

The "standard approach" to tuning is typically achieved by an automated routine where the potential of each electro-optical element or lens is chosen to maximize the measured signal intensity at a selected energy. This tuning energy is commonly chosen to be the most probable energy of the energy distribution. The results of the tuning routine thus define an instrument transmission function that is set by the optimal electro-optical element potentials at the selected energy. The measured ion energy distributions will be the true distributions, only if the transmission function is independent of energy. If instead the transmission function is energy dependent, then the measured distributions will be a convolution of the true distribution and the transmission function. More specifically, if the instrument transmission function is energy dependent, the shape of the measured distributions will vary with the selected tuning energy.

A. Forced-mode energy distributions

Shown in Fig. 2 are the ion energy distributions measured using a *forced-mode* tuning approach. In this approach, the EQP is tuned at a selected incident ion energy and then the full distribution is acquired. Specifically, the energy analyzer was set to pass only those ions of a particular incident energy, and then the count rate was maximized by sequentially adjusting the extractor and lens 1 potentials. For all approaches described in this work, the full range of potentials is scanned for each electro-optical element before moving onto the next electro-optical element. This process virtually guarantees that the signal intensity used is the global maximum, not just a local maximum. The potential values of both the extractor and lens 1 that were used to acquire the distributions of Fig. 2 are plotted in Fig. 3. Also shown in Fig. 3 is the total flux, which was determined by integrating the ion energy distributions of Fig. 2. It should be noted that, for this work, the extractor and lens 1 bias had the largest influence on signal intensity, and the maximum signal varied little with additional tuning of the other ion optics. In other words, the tuning conditions for the other optics were valid for a wide range of extractor bias, lens 1 bias, and incident ion energies.

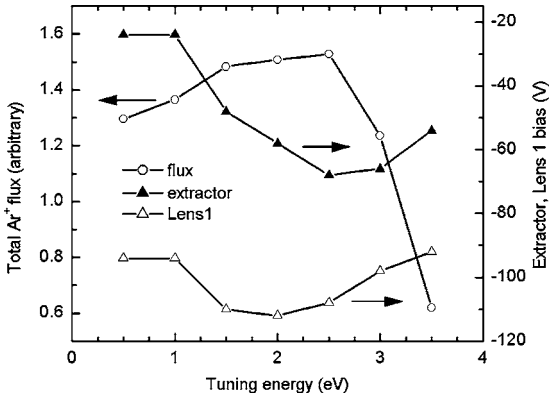

FIG. 3. Total Ar^+ ion flux found by integrating the distributions from Fig. 2 and the optimized electro-optical element biases for each energy.

The results of Figs. 2 and 3 indicate that the transmission function of the EQP depends on the tuning energy. As a result, the distribution obtained with a tuning energy of 2.5 eV, which is the most probable energy, does not accurately reflect the true distribution. While this distribution optimizes the critical metrics (peak intensity and total flux), it clearly differs in structure compared to distributions produced using different tuning energies, particularly at the low-energy end of the distributions.

Shown in Fig. 4 are the results using a similar approach except that for these, both the tuning energy and the extractor bias were held constant and only the lens 1 potential was

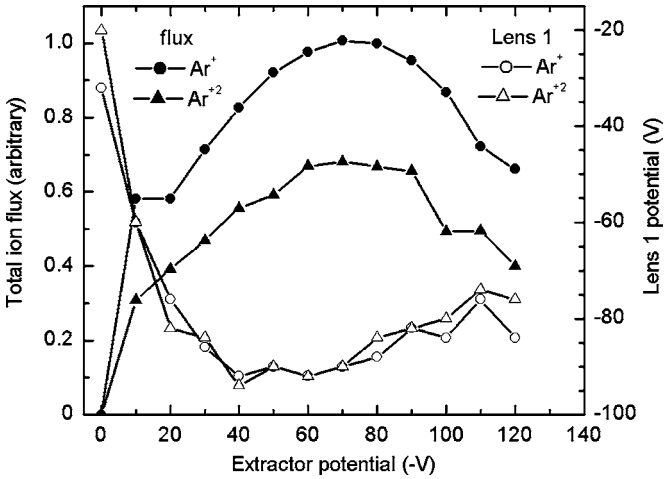

FIG. 4. Total Ar^+ and Ar^{+2} ion fluxes as a function extractor bias. Also shown are the lens 1 biases that maximize the ion flux for each extractor bias.

Downloaded 20 Aug 2007 to 132.250.158.37. Redistribution subject to AIP license or copyright, see http://rsi.aip.org/rsi/copyright.jsp

optimized with respect to the ion signal. For Ar^+ the tuning energy was 3.3 eV (6.6 eV for Ar^{+2}) and the extractor bias was selected as indicated. These measurements were performed for both Ar^+ and Ar^{+2} ions and the results were similar, in that the total flux was optimized at a similar extractor bias and the lens 1 values were similar. The inclusion of Ar^{+2} was useful in ensuring that the conditions were valid for ions sampled from the plasma and not those generated inside the EQP; there are no gas-phase reactions that could generate Ar^{+2} within the instrument.

B. Energy-tuned distributions

The results of Figs. 2–4 indicate the optimal extractor and lens 1 bias vary as function of ion energy, and thus an energy-dependent tuning function must be considered when acquiring ion energy distributions. This led to the development of an *energy-tuned* approach, which incorporated the optimization procedure described above *into* the acquisition of the energy distribution. That is, the signal intensity was determined by sequentially optimizing the extractor and lens 1 potential, for each value of ion energy as the energy was stepped from its minimum value (typically zero) to its maximum value. In contrast to the forced-mode method in which tuning is performed at one incident energy prior to acquiring the distribution, the energy-tuned method optimizes the signal intensity at each energy as the full distribution is measured. The software allows the procedure to be automated so that the data were acquired for the entire energy range without any user input. The results of this energy-tuned approach are shown in Figs. 5–7 for a variety of operating conditions. The distributions of Fig. 5 were acquired during a 4–6 ms wide gate at the end of the electron beam pulse, while the distributions of Fig. 6 included all phases of plasma production. The results of Fig. 7 were also taken during a 4–6 ms wide gate at the end of the pulse, but the plasma potential was elevated by biasing the termination anode to +5 V, thus producing a wider range of incident ion energies.

Included in Figs. 5–7 are the optimum values of the extractor and lens 1 potentials at the specified energy. These values are selected prior to the start of the energy scan, but are reset to the optimum values after scanning the extractor and lens 1, provided the intensity is above 500 counts/s (the default value set by the manufacturer). Since the signal intensity naturally falls to zero at energies above the plasma potential, a considerable variation in electro-optical element values is observed at high energies.

A comparison of the standard method, a convolution of the forced-mode results, and the energy-tuned method is shown in Fig. 8. The convolution is simply a sum of all the distributions in Fig. 2. For ease in comparison, all distributions of Fig. 8 were normalized to their respective peak intensities. The difference in relative intensities is apparent, with most of difference occurring between threshold and the most probable energy (2.5 eV). In terms of total flux, the energy-tuned approach gives the largest flux, with the forced-mode convolution and standard approach lagging by 4% and 8%, respectively, for the 4–6 ms gate and by 12% and 14% for the distributions acquired over all time.

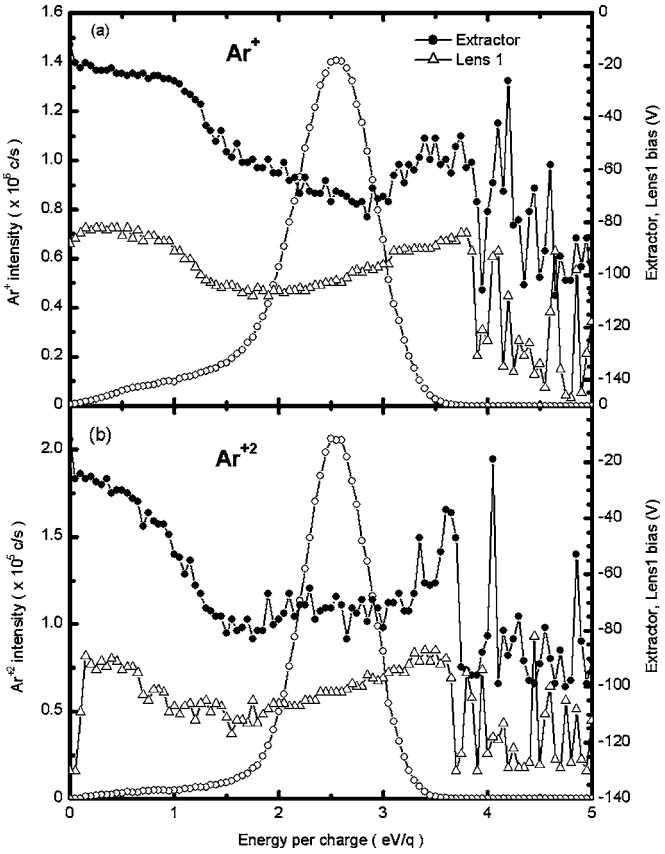

FIG. 5. Energy-tuned approach for (a) Ar^+ and (b) Ar^{+2} distributions acquired over the last 2 ms of the pulse. Also shown are the optimized electro-optical element biases that yield the intensity at each energy of the distribution.

C. Simulations

Two energies, 0.5 and 2.5 eV, were used in these simulations and were chosen to agree with the very different tuning conditions and flux measurements shown in Fig. 6. The electro-optical element potentials were also chosen to roughly agree with the extractor and lens 1 values in Fig. 6, and the values used for other optics were taken from the experimental conditions. For each energy, two separate variations in the ion trajectories were simulated. The first set of trajectories was launched from the center of the orifice but varied in angle over a range of ±26° with respect to the axis normal. The second set of trajectories spanned the orifice diameter but remained at normal incidence. We use the term "acceptance angle" to describe the solid angle over which ions are accepted and the term "acceptance area" to describe the area determined by the ions farthest from the orifice center that were accepted.

Generally, the results showed that for both energies, an increase in extractor voltage resulted in an increase in the acceptance angle but a decrease in acceptance area. The results also indicate that higher ion energies require higher voltages. More specifically, if the ion is on axis and has a large angle of incidence, a greater extractor voltage is required to collect that ion. On the other hand, if the ion is at normal incidence but off axis, a larger extractor voltage causes the ion to be missed.

Downloaded 20 Aug 2007 to 132.250.158.37. Redistribution subject to AIP license or copyright, see http://rsi.aip.org/rsi/copyright.jsp

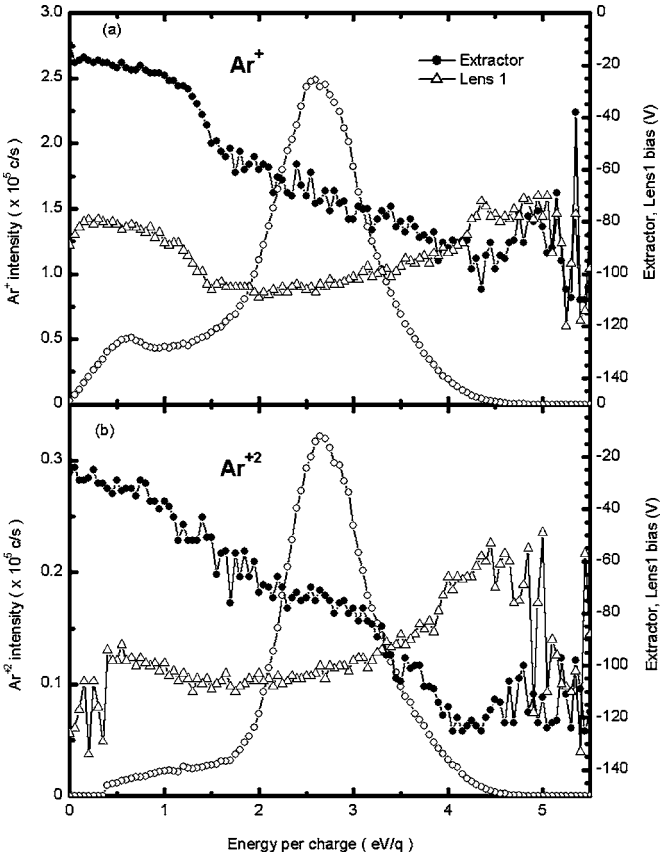

FIG. 6. Energy-tuned approach for (a) Ar^+ and (b) Ar^{+2} distributions acquired over the entire plasma period along with the optimized electro-optical element biases.

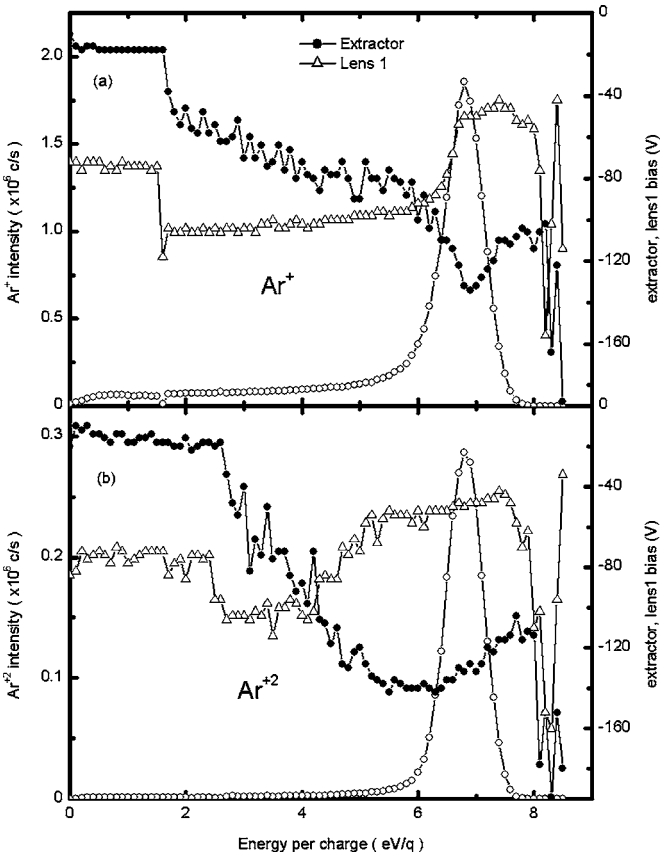

FIG. 7. Energy-tuned approach for (a) Ar^+ and (b) Ar^{+2} distributions acquired during the last 2 ms of the pulse and the termination anode is biased to +5 V. Also shown are the optimized electro-optical element biases.

IV. DISCUSSION

The results presented suggest that the instrument transmission function depends on the incident ion energy and is largely determined by the extractor and lens 1 potentials. Experiments that utilize a low-energy ion source could be used to independently verify this result and determine its cause. Unfortunately, the authors are unaware of an ion source with the energy range and resolution required for such measurements. The modeling results do, however, provide insight as to why the device operates in the manner determined using the energy-tuned approach.

One possible cause for the energy-dependent transmission function is related to the angular spread in ions as they enter the EQP. The incident angle may be larger at lower energies from either collisions within the sheath or field distortions at the orifice. This type of energy dependence, however, is not supported in this work. The modeling results show that a larger extractor potential is required to increase the acceptance angle at all energies, while the experimental results showing an increase in extractor potential is required as the ion energy increases. These two results are not compatible with each other if one assumes that the anisotropy increases with increasing energy. It is plausible, however, to assume that the anisotropy of the ion flux is fairly constant over the range of energies if one considers the following: In the distributions of Fig. 6, where the data were taken over all the phases of plasma production, the spread in energy is largely caused by a time-dependent plasma potential and not necessarily by collisions within the sheath. Even in the case of the steady state (Fig. 5) measurements, there is no reason to assume that the angular spread in the incident ion flux is significantly increased due to collisions.[10,18] Moreover, using a plasma density of 10^{10} cm^{-3} at the electrode face and an electron temperature of 1 eV, the Debye length is estimated to be 75 μm and so, the orifice diameter (20 μm) is small enough that perturbations at the entrance are minimal.[7]

The modeling results do show that a low extractor voltage at low ion energies is required to maintain a large acceptance area, which is consistent with the data if one assumes that virtually all the ions are highly anisotropic. Low bias on the extractor minimizes the field gradients around the entrances of the extraction region, thus causing less deflection of the low-energy ions at normal incidence. At higher ion energy, larger potentials can be tolerated.

Overall, the simulations indicate that the energy-tuned technique is an improved way to measure the ion energy distributions by adjusting the extractor and lens 1 potentials to maximize, in combination, the acceptance angle and area. That is, while the acceptance angle and acceptance area might not be optimized separately, they are as a whole.

Barton *et al.*[19] previously explored a similar approach when measuring ion energy distributions in a rf discharge. In that work, they describe reconstructing the energy distribution from a group of distributions measured over a fraction of the total energy range. Specifically, the signal was opti-

Downloaded 20 Aug 2007 to 132.250.158.37. Redistribution subject to AIP license or copyright, see http://rsi.aip.org/rsi/copyright.jsp

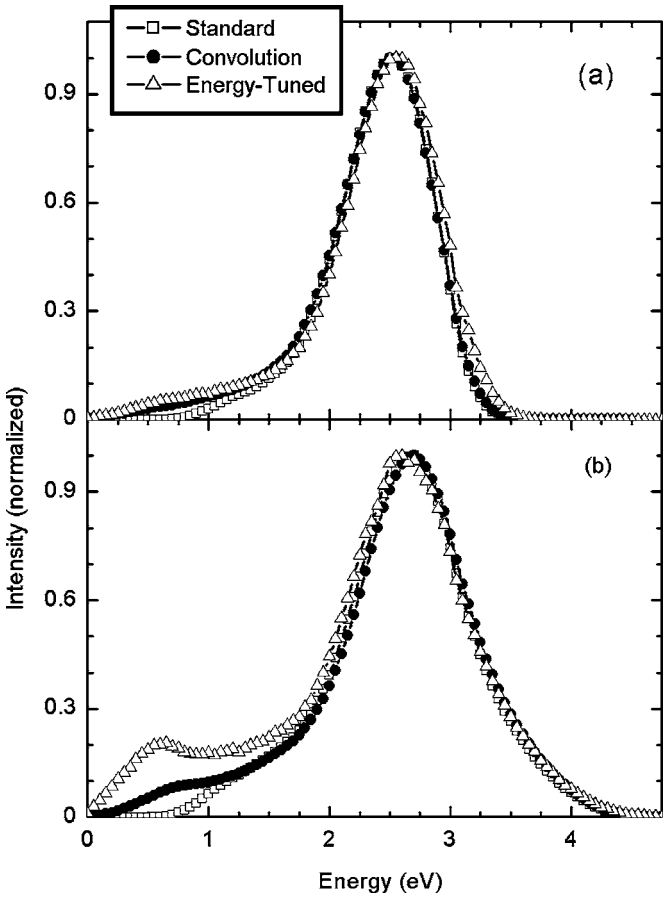

FIG. 8. A comparison of Ar^+ ion energy distribution measurement approaches acquired during the (a) steady state (4–6 ms) and (b) nearly the entire period (0–27 ms).

mized at a selected energy and the intensity was measured over a 2 eV range centered about the tuning energy and then repeated in 2 eV increments. The entire distribution was then constructed by summing the intensities measured over the 2 eV intervals. The energy-tuned method described in the present work is similar but more exact, since no assumptions need to be made with respect to the range over which the tuning conditions are valid.

The accuracy of the technique is difficult to assess since the true distributions are unknown. However, the energy-tuned approach has been used previously[12] to develop a temporal description of pulsed plasmas, and the results were found to correlate well with Langmuir probe diagnostics and a first principles theoretical description of the ion flux. We further note that the similarity in tuning conditions for Ar^+ and Ar^{+2} ions is encouraging. Since Ar^{+2} must originate inside the plasma, it is reasonable to assume that all Ar^+ ions being sampled come from the plasma as well, and thus the low-energy part of the distribution is not an artifact of charge exchange reactions within the EQP.

The energy-tuned approach does have the disadvantage of increasing the time required to accumulate each distribution, which will vary with the number of energy steps chosen. When considering its use, this drawback should be weighed against the improved collection efficiency, which for these experiments was found to increase the measured flux by as much as 20%.

V. SUMMARY

This work describes a method to acquire ion energy distributions using a dual energy analyzer/mass spectrometer (EQP 300) manufactured by Hiden Analytical. The method incorporates signal optimization into the acquisition of the ion energy distribution such that the signal is optimized for each energy increment. The results were compared to the standard approach where the signal optimization is carried out for a single energy, often the most probable energy of the ion energy distribution. Simulations indicate that the new method improves the collection of low-energy ions and thus provides a more accurate measure of the ion energy distribution. Although this method was developed using a specific instrument, the approaches described in this work could be applied to any similarly constructed device that samples ion species from a plasma through a small orifice.

ACKNOWLEDGMENTS

The authors appreciate the many useful conversations with Dr. Alan Rees, Dr. Claire Greenwood, and Dr. Yolanda Gonzalvo of Hiden Analytical, Inc. This work was supported by the Office of Naval Research.

[1] J. W. Coburn, Rev. Sci. Instrum. **41**, 1219 (1970).
[2] The ion energy distributions measured by these devices are not total energy distributions since only the forward component of the velocity distributions is measured and these systems are limited to sampling a narrow angular distribution. K. Ellmer, R. Wendt, and K. Wiesemann, Int. J. Mass. Spectrom. **223–224**, 679 (2003).
[3] L. Tonks, H. M. Mott-Smith, and I. Langmuir, Phys. Rev. **28**, 104 (1926).
[4] H. Helm, F. Howorka, F. Handle, F. Egger, and W. Lindinger, J. Phys. B **7**, 170 (1974).
[5] J. W. Coburn and E. Kay, J. Vac. Sci. Technol. **8**, 738 (1971).
[6] J. Liu, G. L. Huppert, and H. H. Sawin, J. Appl. Phys. **68**, 3916 (1990).
[7] C.-K. Kim and D. J. Economou, J. Appl. Phys. **91**, 2594 (2002).
[8] J. S. Kim, M. V. V. S. Rao, M. A. Cappelli, S. P. Sharma, and M. Meyyappan, Plasma Sources Sci. Technol. **10**, 191 (2001).
[9] J. K. Olthoff, R. J. Van Brunt, S. B. Radovanov, J. A. Rees, and R. Surowiec, J. Appl. Phys. **75**, 115 (1994).
[10] J. Janes and C. Huth, J. Vac. Sci. Technol. A **10**, 3522 (1992).
[11] S. G. Walton, D. Leonhardt, D. D. Blackwell, R. F. Fernsler, D. P. Murphy, and R. A. Meger, J. Vac. Sci. Technol. A **19**, 1325 (2001).
[12] S. G. Walton, D. Leonhardt, and R. F. Fernsler, IEEE Trans. Plasma Sci. **33**, 838 (2005).
[13] D. Leonhardt, C. Muratore, S. G. Walton, and R. A. Meger, Surf. Coat. Technol. **188–189**, 299 (2004).
[14] W. M. Manheimer, R. F. Fernsler, M. Lampe, and R. A. Meger, Plasma Sources Sci. Technol. **9**, 370 (2000).
[15] Hiden Analytical Ltd., Warrington WA5 7UN, U.K.
[16] This information was provided by the manufacturer. Note that the device is commonly operated at a $E_t \approx 40$ eV with a $\Delta E \approx 1.0$ eV.
[17] D. A. Dahl, J. E. Delmore, and A. D. Appelhans, Rev. Sci. Instrum. **61**, 607 (1990).
[18] A. V. Phelps, J. Appl. Phys. **76**, 747 (1994).
[19] D. Barton, D. J. Heason, R. D. Short, and J. W. Bradley, Meas. Sci. Technol. **11**, 1726 (2000).

Downloaded 20 Aug 2007 to 132.250.158.37. Redistribution subject to AIP license or copyright, see http://rsi.aip.org/rsi/copyright.jsp